Volume 7 | Number 19 | 7 October 2023

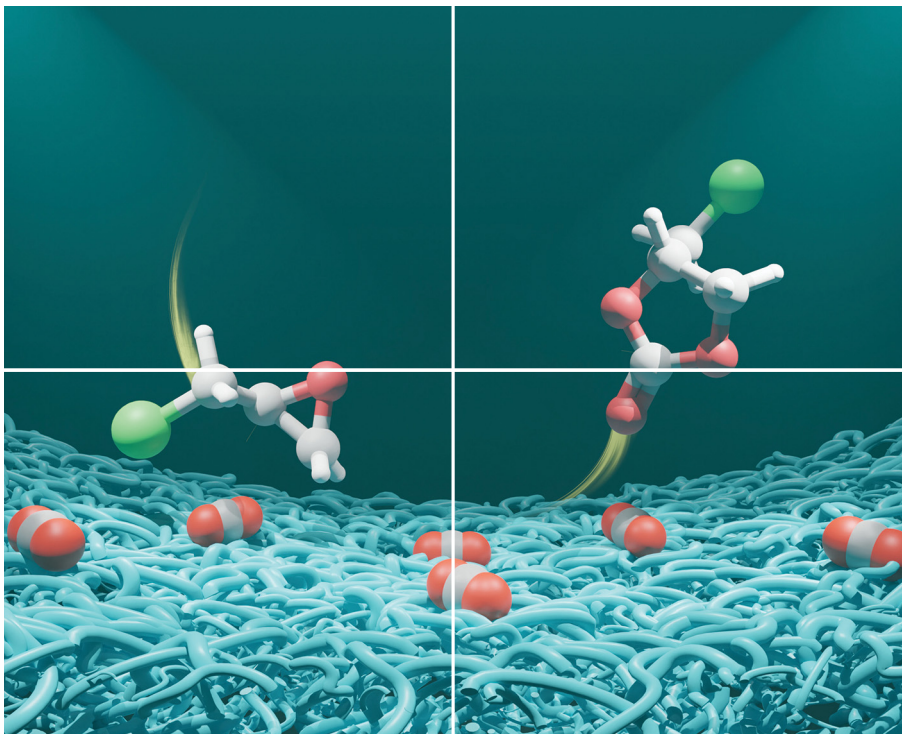

MATERIALS CHEMISTRY

FRONTIERS

CCS 中国化学会 CHINESE CHEMICAL SOCIETY

ICCAS 1956

ROYAL SOCIETY OF CHEMISTRY

rsc.li/frontiers-materials

MATERIALS CHEMISTRY FRONTIERS

RESEARCH ARTICLE

View Article Online
View Journal | View Issue

Cite this: *Mater. Chem. Front.*, 2023, **7**, 4473

Bifunctional metal-free porous polyimide networks for CO_2 capture and conversion†

Basiram Brahma Narzary, Ulzhalgas Karatayeva, Jerry Mintah, Marcos Villeda-Hernandez and Charl F. J. Faul *

Received 5th June 2023,
Accepted 13th August 2023

DOI: 10.1039/d3qm00639e

rsc.li/frontiers-materials

Carbon dioxide (CO_2) capture and conversion into valuable chemicals is a promising and sustainable way to mitigate the adverse effects of anthropogenic CO_2 and climate change. Porous polyimides (pPIs), a class of highly cross-linked porous organic polymers (POPs), are promising candidates for CO_2 capture as well as catalytic conversion to valuable chemicals. Here, two metal-free perylene-based pPIs were synthesised *via* polycondensation reaction. The pPIs exhibit excellent heterogeneous catalytic activities for cycloaddition of CO_2 to epoxides under very mild and sustainable conditions (slight CO_2 overpressures, solvent- and co-catalyst free at 80 °C) with 98% conversion. The effects of reaction conditions, such as reaction temperature, reaction time and catalyst loading on the cycloaddition performance were investigated. Moreover, the pPIs can be recycled and reused five times without a substantial loss of catalytic activity. Furthermore, these materials were used in the electroreduction of CO_2 to form formate and methanol with faradaic efficiencies (FEs) of 20% and 95%, respectively, in the applied potential range from 0 to −1 V *vs.* RHE.

1. Introduction

Climate change is the most significant challenge humanity is facing in the 21st century, caused by continuously increasing human activity, leading to excessive anthropogenic CO_2 emissions. However, CO_2 has the potential to be used as a very abundant, inexpensive, and non-toxic source of carbon for industrial utilisation.[1,2] Therefore, capturing and converting CO_2 into useful chemical feedstocks offer an important emerging approach to developing a carbon-neutral alternative to fossil fuel resources.[3,4]

From a sustainability perspective, CO_2 can be transformed into cyclic carbonates *via* the cycloaddition reaction between carbon dioxide and epoxides,[5] and be photochemically[6] and electrocatalytically[7] reduced to valuable chemicals and fuels. Cyclic carbonates are industrially important and used in a wide range of applications, including as building blocks for polymeric materials,[8] solvents,[9] and, importantly, as electrolytes for lithium ion batteries.[10] Additionally, photochemical and electrochemical reduction of CO_2 can lead to the production of highly desirable C1, C2, and higher carbon products.[6,7] To date various heterogeneous catalytic systems, including transition metals, have been developed and extensively researched for CO_2 conversion.[11,12] However, the use of metal catalysts is limited due to their high cost, uncertainty in terms of long-term availability and sustainability, poor selectivity, low durability, susceptibility to gas poisoning, and negative environmental impact, hindering their application in industry.[13] To overcome the limitations of traditional metal catalysts, a variety of metal-containing porous materials, specifically covalent–organic frameworks (COFs),[14,15] and metal–organic frameworks (MOFs),[16,17] have been widely explored as effective CO_2 sorption materials, and, more recently, also as materials for conversion. However, many obstacles remain in the development of the CO_2 capture and conversion processes, including the design of stable and metal-free materials with high CO_2 adsorption abilities and selectivity, effective CO_2 conversion under benign conditions, affordability and recyclability.

pPIs are an interesting class of metal-free highly cross-linked porous materials that have shown promising results for CO_2 capture owing to their high porosity, synthetic flexibility, and excellent physical and chemical properties.[18] Based on these attractive properties, the applications of pPIs have been extensively explored in the fields of gas capture and storage,[19,20] energy storage,[21–24] sensing,[20,25] drug delivery[26] and functionalised coatings.[27]

Post-synthetic modification of pPIs with metal species (Pd and Cu) have been explored for use as heterogeneous catalysts, including for Suzuki coupling reactions,[28,29] and aerobic oxidation of benzyl alcohol.[30] However, the route to transforming CO_2 (chemically and electrocatalytically) into value-added chemicals has not been explored to date for metal-free pPIs, despite their high CO_2 affinities. These high affinities, stemming from abundant heteroatomic active sites in their structure, have

School of Chemistry, University of Bristol, Bristol, BS8 1TS, UK.
E-mail: charl.faul@bristol.ac.uk

† Electronic supplementary information (ESI) available. See DOI: https://doi.org/10.1039/d3qm00639e

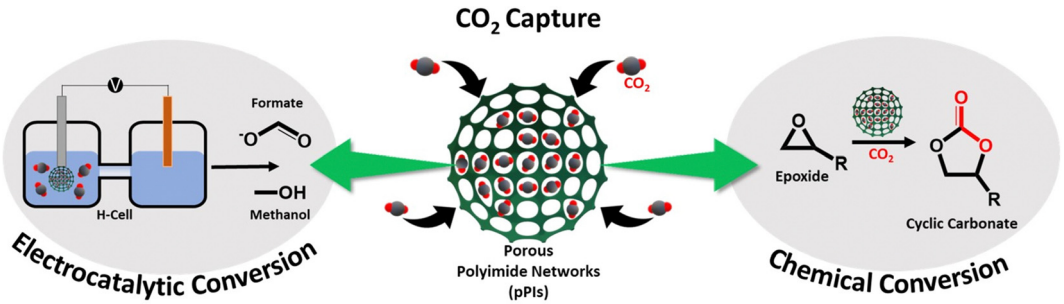

Scheme 1 Sustainable routes to CO_2 capture and conversion using pPIs.

been shown to yield enhanced interactions in both electro- and chemo-catalytic processes.[31,32] The mobility of electrons, required for such catalytic processes, can furthermore be facilitated by the presence of conjugated structures within the backbone, especially if an organic semiconductor is incorporated. We have recently shown the validity of this approach for the case of poly(naphthalene imide)s, specifically for the electrocatalytic reduction of CO_2 to formate and methanol.[33] Here we explore the use of perylene tetracarboxylic dianhydride (**PTCDA**) as a further well-known example of suitable conjugated materials for such approaches.[34]

In this investigation, we explore the use of perylene-based pPIs, for the first time, at standard pressures as metal-free heterogeneous catalysts for incorporating CO_2 in epoxides to form cyclic carbonates, as well as for electrocatalytic CO_2 conversion into valuable fuels and feedstocks (see Scheme 1).

2. Results and discussion

pPI-1 and **pPI-2** were obtained by polycondensation of **PTCDA** with melamine and tris-(4-aminophenyl)triazine (**TAPT**), respectively (Scheme 2). The successful formation of both pPIs was confirmed by Fourier-transform infrared spectroscopy (FT-IR), ultraviolet-visible near-infrared spectroscopy (UV-Vis-NIR), thermogravimetric analysis (TGA), powder X-ray diffraction (PXRD), scanning electron microscope (SEM), energy-dispersive X-ray spectroscopy (EDX) and X-ray photoelectron spectroscopy (XPS) as shown in Fig. 1(a–f) and Fig. S9, S10 and Table S1 (ESI†). The characteristic FT-IR absorption signals at 1773 and 1707 cm^{-1} are attributed to the symmetric and asymmetric vibrations, characteristic of carbonyl groups in the newly formed six-membered polyimide rings of **pPI-1** and **pPI-2**. Additionally, the absence of –NH stretching signals (3460–3213 cm^{-1}) from the starting material shows complete condensation of amine moieties to form the respective pPI. The signal at 1446 cm^{-1} confirms the presence of triazine units in both polymers. The maximum UV-Vis-NIR absorption wavelength (λ_{max}) of **pPI-1** and **pPI-2** are 733 and 764 nm, respectively, with absorption features extending beyond 1400 nm, indicating the formation of new products (Fig. 1d). The amorphous nature of **pPI-1** and **pPI-2** was confirmed by PXRD measurements, with broad peaks at 12.5°, commonly observed for POPs.[20] A further broad peak centred around 26° originates from π–stacking between the aromatic units (Fig. 1c).[20] Thermogravimetric studies under nitrogen (N_2) atmosphere revealed degradation temperatures (T_{dec}) of 400 °C and 590 °C, with 45% and 70% char yields at 800 °C, respectively, for **pPI-1** and **pPI-2**, confirming the excellent thermal stability of these pPIs.

The porosity properties of pPIs were investigated by recording N_2 sorption isotherms at 77 K (see Fig. S4, ESI†). The isotherms show no significant N_2-uptake at lower relative pressures (P/P_0), with some uptake observed at higher relative pressures (P/P_0). This behaviour indicates the presence of micro- and macropores, as

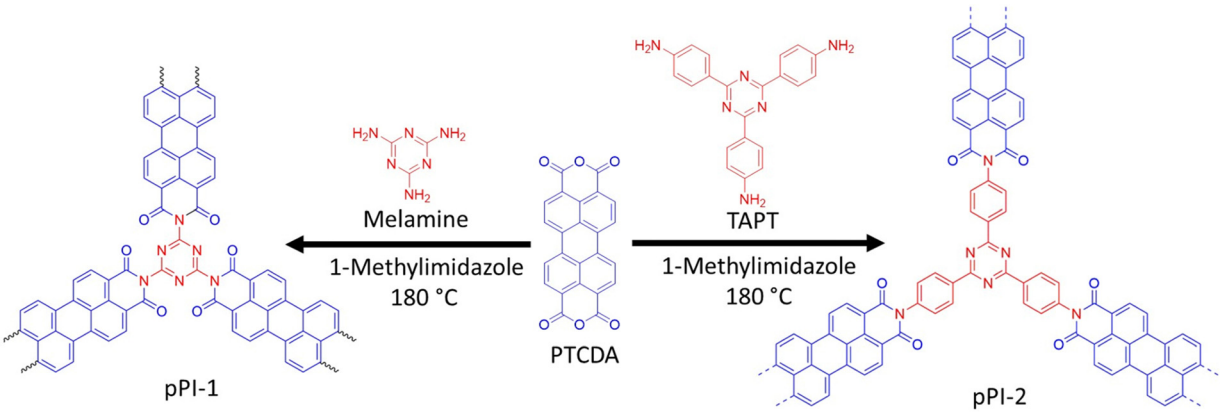

Scheme 2 Synthetic pathway to **pPI-1** and **pPI-2**.

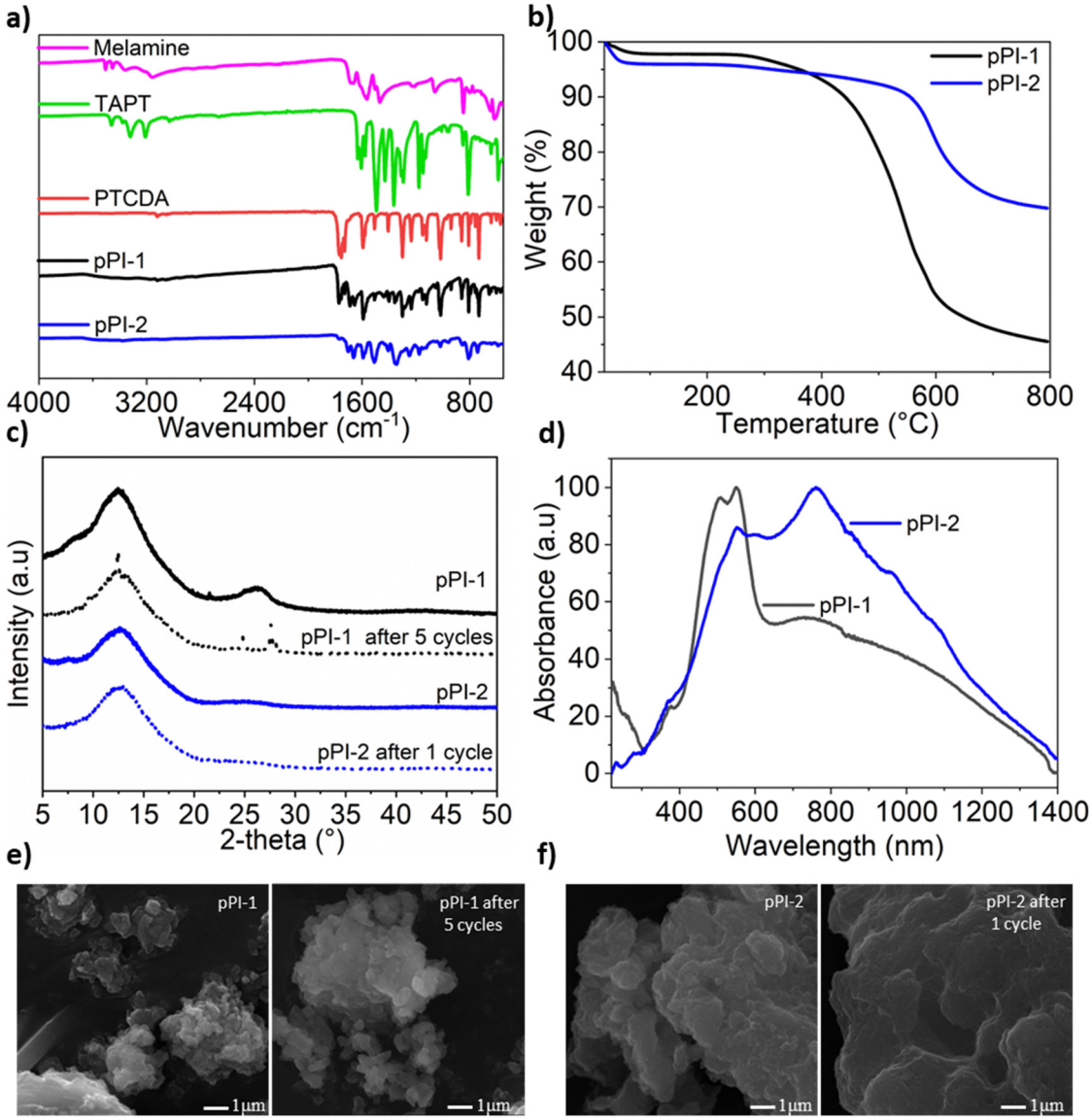

Fig. 1 (a) FT-IR spectra of starting materials and **pPI-1** and **pPI-2**, (b) TGA plot of **pPI-1** and **pPI-2** under N_2 atmosphere, (c) PXRD of **pPI-1** and **pPI-2** (solid line) and after use as a catalyst (dotted line) (peak 2θ 21.5 is from the paraffin wax used to fix samples to the sample holder during our XRD analysis),[35] (d) UV-Vis-NIR spectra of **pPI-1** and **pPI-2**, (e) SEM of **pPI-1** before and after 5 cycles used as a catalyst, and (f) SEM micrographs of **pPI-2** before and after 1 cycle used as a catalyst.

confirmed in pore size distribution (PSD) calculations using the non-local density functional theory (NL-DFT) method (see Fig. S4, ESI†).[20] These isotherms could be described as typical Type II isotherms according to the IUPAC classification,[36] with the specific surface areas (S_{BET}) of **pPI-1** and **pPI-2**, 20 and 342 $m^2\ g^{-1}$, respectively. Additionally, the CO_2 uptake capabilities of the pPIs were investigated at 273 K (2 wt% and 5 wt% for **pPI-1** and **pPI-2**, respectively) and 298 K (0.8 wt% and 3 wt% for **pPI-1** and **pPI-2**, respectively) at 1 bar pressure (see Table 1 for full details). Even though **pPI-1** exhibits poor S_{BET} surface area, the relatively high CO_2 uptake of this polymer may be attributed to the strong affinity between its constituent heteroatoms and CO_2.[37,38] To quantify the interaction between the pPIs and CO_2, the isosteric heats of adsorption (Q_{st}) were calculated from the absolute adsorption isotherms recorded at 273 and 298 K (Table 1). The highest adsorption enthalpies of **pPI-1** and **pPI-2** are 39 kJ mol^{-1} and 30 kJ mol^{-1}, respectively, as shown in Table 1. These values indicate physisorption processes and interactions for both of these polymers with CO_2. Interestingly, **pPI-1** has stronger CO_2–surface interactions (Q_{st} 39 kJ mol^{-1}), thus resulting in moderate

Table 1 Porosity parameters and CO_2 uptake at 273 K and 298 K at 1 bar

			CO_2 uptake (wt%)		
Polymer	S_{BET} ($m^2\ g^{-1}$)	PV ($cm^3\ g^{-1}$)	273 K	298 K	Q_{st} (kJ mol^{-1})
pPI-1	20	0.07	2.0	0.8	39
pPI-2	342	1.12	4.9	3.0	30

CO_2 uptake, even with a surface area (20 m^2 g^{-1}) 17 times lower when compared with **pPI-2** (342 m^2 g^{-1}).

2.1. pPI-catalysed chemical conversion of epoxides

The cycloaddition of CO_2 to epoxides to yield cyclic carbonates is commonly performed using potentially unsuitable metal-containing catalysts (*e.g.*, Zn@SBMMP and Bp-Zn@MA) and under undesirable, energy intensive high temperatures (160 °C) and pressure (~20 bar) conditions.[39–43] The presence of a co-catalyst (*e.g.*, tetrabutylammonium bromide (TBAB)) is also required in most cases, increasing cost and molecular economy.[44,45] The primary driving force behind the cyclic carbonate synthesis from CO_2 and epoxide is substrate activation. Several studies have already shown that there are three distinct mechanistic pathways: CO_2 activation, epoxide activation, or simultaneous activation of both CO_2 and epoxide.[46–48] The catalyst must have the capability to interact with the substrate and activate it accordingly. Considering the abundant N heteroatoms present in pPIs, we propose that the activation of CO_2 occurs *via* Lewis acid–Lewis base interactions (for detailed plausible mechanisms, refer to ESI† Scheme S1). *In situ* chemical characterisation and computational simulation studies would be beneficial to precisely understand the exact mechanism and interaction between pPIs with CO_2 and epoxide, which however fall outside the scope of this study.

Here we show the successful application of our pPIs, prepared in the absence of any metal-containing catalysts, for the metal-free, solvent-free cycloaddition of CO_2 to epoxides under standard pressure (*i.e.*, using a balloon filled with CO_2). We furthermore find that no co-catalysts are required for quantitative transformation, with all reactions also performed in the absence of solvent (Scheme 3). The well-studied cycloaddition of CO_2 to epichlorohydrin (ECH) was chosen as a benchmark reaction for optimisation. As shown in Table 2, both pPIs efficiently converted ECH to (chloromethyl)ethylene carbonate (CMEC) with a yield of 98% (using **pPI-1**) and 90% (using **pPI-2**), respectively, at 80 °C and after 72 h, in the absence of solvent. Time-dependent analysis of the conversion for both **pPI-1** and **pPI-2** confirmed high conversions only after 72 h, as shown in Fig. 2a and Fig. S5 (ESI†), respectively.

The higher conversion of **pPI-1** could be attributed to the stronger surface interactions with CO_2, as reflected by the Q_{st} value of **pPI-1** (39 kJ mol^{-1}) *vs.* that of **pPI-2** (30 kJ mol^{-1}). To explore the effect of temperature on the resulting yield, the catalysed reaction was carried out at 60, 80 and 100 °C; with the yields plateauing at 98% as shown in Fig. 2b. The catalyst

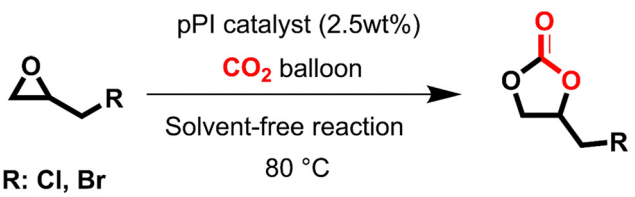

Scheme 3 pPI-catalysed, solvent-free cyclic carbonate synthesis from CO_2 and epoxides.

Table 2 Cycloaddition of CO_2 with different epoxide substrates to form cyclic carbonates using pPIs[a]

Entry	Epoxide	Catalyst	Product	Yield[b] (%)
1		None	None	0
2		**pPI-1**	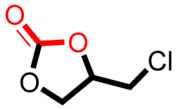	98
3	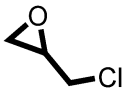	**pPI-2**	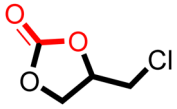	90
4		**pPI-1**	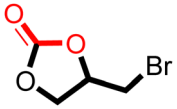	89
5		**pPI-2**	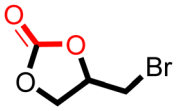	72

[a] Reaction conditions: epoxide (1 mL, neat), pPIs (2.5 wt%), CO_2 (balloon), 80 °C, and 72 h. [b] Determined by ^{1}H-NMR spectroscopic analysis.

loading used in the cycloaddition transformation was initially fixed at 2.5 wt% (30 mg) of catalyst for 1 mL of neat ECH, giving the highest conversion (Fig. 2c). Subsequently, the catalyst loading was increased to 4.8 wt% (60 mg) and 10 wt% (125 mg). Interestingly, even with increased catalyst loading, the transformation of ECH (at 80 °C, over a 72 hour duration) remained unaltered or equivalent to the conversion achieved with 2.5 wt% catalyst loading. Decreased catalyst loading (1.2 wt%) yielded lower transformation (57%). Therefore, 2.5 wt% catalyst loading was selected as the optimum loading during this investigation.

One of the important considerations of heterogeneous catalysts for industrial applications is recyclability.[49,50] Thus, we investigated the recyclability of **pPI-1** in the model reaction, using ECH and CO_2 as reactants. In each cycle, **pPI-1** was recovered by centrifugation, washed and dried before being reused in a repeat reaction with a fresh batch of the ECH substrate. The catalyst was found to be recyclable and reusable for up to five cycles without significant loss in catalytic activity, as shown in Fig. 2d. It was also observed that **pPI-1** retained its amorphous structure after going through 5 catalytic cycles as shown by XRD (Fig. 1c), SEM (Fig. 1e) and chemical composition (see ESI† Table S1 and Fig. S9 for further data and details of the procedure used). EDX revealed an increase in oxygen and carbon content within both pPIs (**pPI-1** and **pPI-2**) after catalysis, indicating the binding of CO_2 to the catalyst. X-ray photoelectron spectroscopy (XPS) supported these findings, showing changes in the oxygen content of the pPIs after catalysis, implying an increase in C–O and/or O–C=O bonds, originating from the reactive CO_2 species (see the ESI† Fig. S10 for XPS results). Cl signals were detected after catalysis, suggesting that the catalyst also interacted with the epoxide substrate

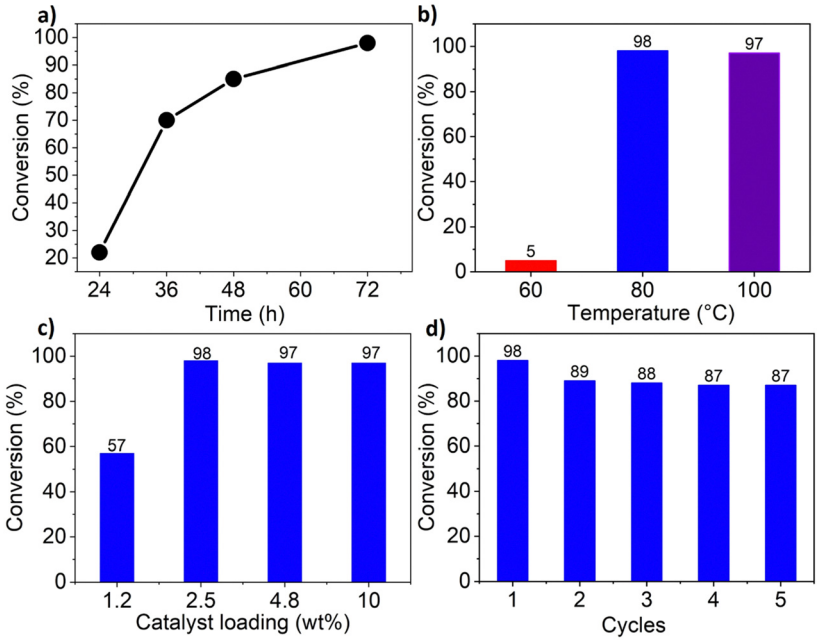

Fig. 2 (a) Time-dependent percentage conversion of ECH at 80 °C for **pPI-1**. (b) Temperature-dependent conversion for cycloaddition of CO_2 to ECH for **pPI-1**. (c) **pPI-1** catalyst loading for cycloaddition of CO_2 to ECH at 80 °C. (d) Recycling test of **pPI-1** for the cycloaddition of CO_2 to ECH at 80 °C.

(ECH). To gain a more precise and detailed understanding of the nature of these interactions between the catalyst, CO_2 and the epoxide, *in situ* chemical characterisation will be part of our future investigations. The potential of using these catalysts in industrial settings is underlined by the physical, chemical and thermal stability, recyclability and lack of obvious changes in catalytic activity or morphology, as also confirmed by additional SEM images recorded post catalysis (see Fig. 1e and f).

After proving the excellent catalytic activity and stability of pPIs for the cycloaddition of CO_2 to ECH, we tested the catalytic performance on a different substrate, epibromohydrin (EBH), under the same reaction conditions (see Table 2). Both pPIs gave excellent conversion (89% and 72%, respectively) of EBH to the corresponding cyclic carbonate.

A number of investigations have been directed towards the production of metal-based catalysts aimed at optimising the conversion of CO_2 into cyclic carbonates.[4] For instance, Zhang *et al.*[51] successfully fabricated cobalt-containing conjugated microporous polymers (CMP) for the cycloaddition of CO_2 and epoxides resulting in 83.6% and 82.5% conversion yields for epichlorohydrin and epibromohydrin, respectively. The same research group later prepared porphyrin-based cobalt-coordinated CMPs for the synthesis of cyclic carbonates from CO_2 and epoxides (with a conversion yield of 74.2% for epichlorohydrin).[52] In both studies, the well-known co-catalyst TBAB was used. Zhou *et al.*[53] reported a zinc (Zn)-containing catalyst for CO_2 transformation; their Zn-salen-CMP successfully converted epichlorohydrin into the corresponding cyclic carbonate with a yield of 89% in the presence of TBAB. Notably, the cycloaddition reaction was carried out at 120 °C and under 3.0 MPa pressure for 1 hour. Another example of using a Zn-containing catalyst, now containing quaternary phosphonium bromide salts, was reported by Lu *et al.*[54] The salts acted in synergy with the zinc porphyrin (Lewis acid) and opened the epoxide ring, eliminating the need for co-catalysts. Reported conversion yields for epichlorohydrin were 93% under high CO_2 pressure (2.5 MPa) at 90 °C. In comparison with metal-based catalysts, there are only a few metal-free POPs for CO_2 fixation *via* cycloaddition of CO_2 with epoxides (but not without a co-catalyst). Ding *et al.*[44] developed microporous polymeric spheres catalyst, which together with TBAB as a co-catalyst gave an 89% conversion yield with epichlorohydrin as a substrate. In contrast to other studies, our results presented here highlight a greener (lower temperatures, pressures and absence of solvents), safer, metal-free alternative for the fixation of CO_2 using a cycloaddition process, using organic-based pPIs only.

2.2. Electrocatalytic CO_2 reduction

To further expand the scope and usage of our pPIs, the electrocatalytic reduction of CO_2 was investigated using a two-compartment H-cell (0.1 M potassium bicarbonate ($KHCO_3$) as the electrolyte in the potential range from −1 to 1 V *vs.* a reversible hydrogen electrode (RHE)). Cyclic voltammetry (CV) studies show that both pPIs exhibit redox activity in the investigated potential range. The CV data (Fig. 3a) shows the current density in the argon-saturated electrolyte is higher than that of the CO_2-saturated electrolyte. The higher current density may be attributed to a higher hydrogen evolution reaction in the argon-saturated electrolyte.[55] Therefore, this data helped to confirm that our pPIs are electrocatalytically active.[55] The chronoamperometric (CA) analyses of these pPIs were carried out at constant potentials of −0.26, −0.56 and −0.76 V *vs.* RHE for 0.5 h (see Fig. 3b and c).

The electrolytes were analysed after electrolysis by cryo-^{1}H NMR, with data shown in Fig. S14 and S15 (ESI†). The measurements

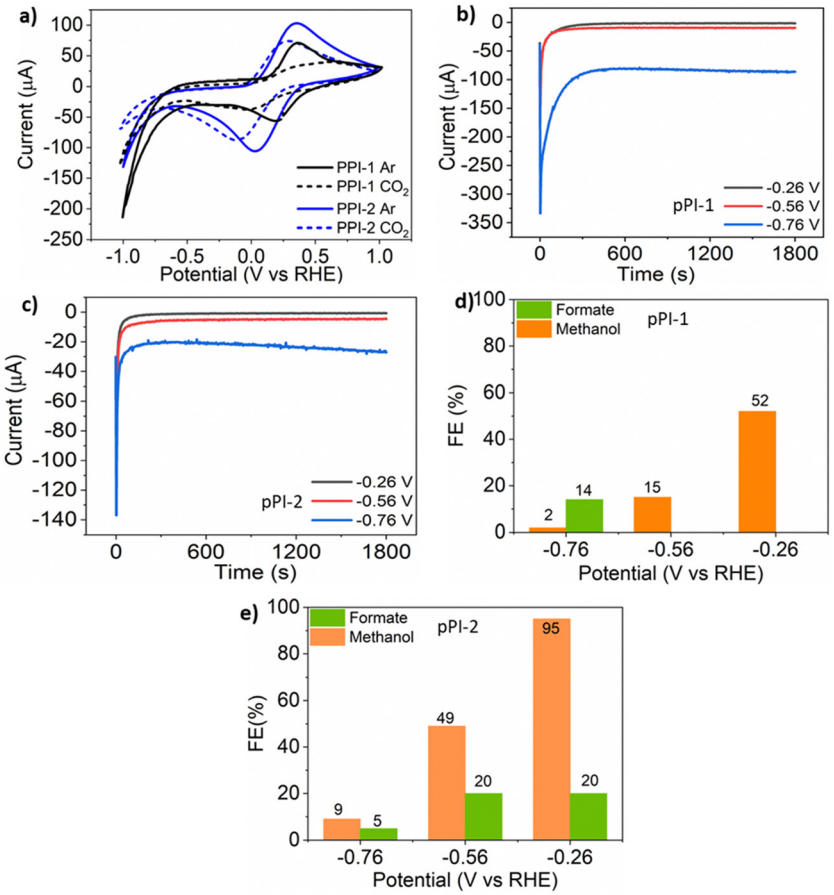

Fig. 3 (a) Cyclic voltammogram of **pPI-1** and **pPI-2** in the applied potential range from −1–1 V *vs.* RHE, scan rate 20 mV s^{-1}, 20 cycles, (b) and (c) chronoamperometry studies (*vs.* RHE) of **pPI-1** and **pPI-2**, respectively in CO_2-saturated electrolytes, and (d) and (e) highest obtained faradaic efficiency of **pPI-1** and **pPI-2**, respectively in CO_2 saturated electrolytes for 30 min.

show that formate and methanol are the primary products present in the CO_2-saturated electrolyte. In the argon-saturated electrolyte, no product signal was detected from samples at the same applied potential as those saturated with CO_2. The signals at 3.36 ppm and 8.50 ppm in the ^{1}H NMR spectra confirm the reduction of CO_2 to methanol and formate, respectively. The stronger Lewis acid–Lewis base interaction of the heteroatoms in the pPIs with CO_2 contributes to increasing the rate of reduction of the gas by stabilising intermediates formed during the conversion.[55] The highest obtained Faradaic efficiency (FE) values are reported in Fig. 3d and e for **pPI-1** and **pPI-2**, respectively (for full data sets, with error bars, see ESI† Fig. S13). **pPI-1** demonstrates a FE of up to 52% for methanol and 14% for formate at −0.26 and −0.76 V *vs.* RHE, respectively, as illustrated in Fig. 3d. For detailed FE calculations, please refer to Section 4 of the ESI.† **pPI-2**, in contrast, exhibits the highest FE for methanol, reaching up to 95% at −0.26 V *vs.* RHE (Fig. 3e). However, the FE gradually decreases with increasing negative potential, with values of 49% at −0.56 V and 9% at −0.76 V, as shown in Fig. 3e. Moreover, **pPI-2** was also capable of reducing CO_2 to formate at −0.26 V (FE = 20%), −0.6 V (FE = 20%) and −0.76 V (FE = 5%). The higher FE of **pPI-2** for methanol could be attributed to the higher surface area and broad PSD, leading to higher carbon product formation. This observation aligns with the findings from our previous study.[33] Additionally, we assume that gaseous products, such as CO and CH_4, formed during the electroreduction process. However, this assumption could not be confirmed since the reaction setup was not coupled with a GCMS instrument. Investigating this aspect further in future research would be of great interest. Multiple metal-based COF and MOF catalyst systems have been used in electrocatalytic CO_2 reduction, reporting outstanding FEs for CO (97% at −0.9 V *vs.* RHE).[56,57] To the best of our knowledge, selectively reducing CO_2 electrocatalytically to methanol using metal-based porous materials has not been achieved to date. In contrast, the pPIs herein reported show superior results for methanol production, and in some cases matching with other traditional transition-metal electrocatalysts (FEs of 87% and 98% for methanol and formate, respectively).[58,59] Our new approach here points towards the exciting development of metal-free porous polymers as electrocatalysts for the wide and sustainable utilisation of CO_2.

3. Conclusion

In this work, two perylene-based pPIs were successfully synthesised *via* polycondensation reactions. The synthesized pPIs

were shown to be versatile materials, showing interesting porosity properties and useful CO_2 uptake capabilities of up to 4.9 wt%. The synthesised pPIs were furthermore successfully utilised, not only to capture CO_2 but also to act as heterogeneous catalysts for the utilisation of CO_2 under very mild and sustainable conditions. **pPI-1** and **pPI-2** showed excellent catalytic performance for cyclic carbonates synthesis from CO_2 and epoxides (at very slight CO_2 overpressures, in the absence of solvents and co-catalysts), with up to 98% conversion and outstanding recyclability. Further exploring their versatility, these pPIs were used in the electrocatalytic conversion of CO_2 to form methanol and formate. FEs of 20% for formate and 95% for methanol were achieved in the applied potential range from 0 to −1 V *vs.* RHE. pPIs, therefore, provide an exciting, metal-free solution, at low potentials, for the electrocatalytic conversion and fixation of CO_2 to produce useful fuels and chemical feedstocks. This approach should therefore continue to be explored to produce efficient and recyclable heterogeneous catalysts for chemical and electrocatalytic conversion of CO_2. Further investigations, based on our earlier work on exploiting and optimising Hansen Solubility Parameters (HSPs) in the Bristol-Xi'an Jiaotong (BXJ) approach, will be useful to explore the influence of the formation of highly optimised conjugated microporous polymers (CMPs). Applying this approach, we will be able to tune porosities and pore size distributions, thereby further improving catalytic efficiency and functionality, and potentially also tune product formation.[60,61] This metal-free, solvent-free approach will ensure a step-change in the approaches and tools available to address the significant global challenges faced today.

Conflicts of interest

There are no conflicts to declare.

Acknowledgements

B.B.N acknowledges support from the National Overseas Scholarship for ST Students, Government of India. U.K. acknowledges support from the Bolashak International Scholarship. J.M. acknowledges support from the Henry Royce Institute. M.V-H acknowledges Bristol Centre for Functional Nanomaterials and the Consejo Nacional de Ciencia y Tecnología (CONACyT, MX) grant no. 497607 for funding and C. F. J. F. acknowledges EPSRC EP/R511663/1 for support. Authors acknowledge access to the Bristol NanoESCA Facility under EPSRC Strategic Equipment Grant EP/M000605/1. The authors thank John Worth and Maximilian Hagemann for proofreading.

References

1 M. M. F. Hasan, L. M. Rossi and D. P. Debecker, *et al.*, Can CO_2 and Renewable Carbon Be Primary Resources for Sustainable Fuels and Chemicals?, *ACS Sustainable Chem. Eng.*, 2021, **9**(37), 12427–12430, DOI: 10.1021/acssuschemeng.1c06008.
2 Q. Liu, L. Wu, R. Jackstell and M. Beller, Using carbon dioxide as a building block in organic synthesis, *Nat. Commun.*, 2015, **6**(1), 5933, DOI: 10.1038/ncomms6933.
3 P. Bhanja, A. Modak and A. Bhaumik, Porous Organic Polymers for CO_2 Storage and Conversion Reactions, *ChemCatChem*, 2019, **11**(1), 244–257, DOI: 10.1002/cctc.201801046.
4 K. S. Song, P. W. Fritz and A. Coskun, Porous organic polymers for CO_2 capture, separation and conversion, *Chem. Soc. Rev.*, 2022, **51**(23), 9831–9852, DOI: 10.1039/D2CS00727D.
5 L. Guo, K. J. Lamb and M. North, Recent developments in organocatalysed transformations of epoxides and carbon dioxide into cyclic carbonates, *Green Chem.*, 2021, **23**(1), 77–118, DOI: 10.1039/D0GC03465G.
6 T. Kong, Y. Jiang and Y. Xiong, Photocatalytic CO_2 conversion: What can we learn from conventional CO x hydrogenation?, *Chem. Soc. Rev.*, 2020, **49**(18), 6579–6591, DOI: 10.1039/C9CS00920E.
7 L. Li, X. Li, Y. Sun and Y. Xie, Rational design of electrocatalytic carbon dioxide reduction for a zero-carbon network, *Chem. Soc. Rev.*, 2022, **51**(4), 1234–1252, DOI: 10.1039/D1CS00893E.
8 C. Ngassam Tounzoua, B. Grignard and C. Detrembleur, Exovinylene Cyclic Carbonates: Multifaceted CO_2 -Based Building Blocks for Modern Chemistry and Polymer Science, *Angew. Chem., Int. Ed.*, 2022, **61**(22), e2021160, DOI: 10.1002/anie.202116066.
9 B. Schäffner, F. Schäffner, S. P. Verevkin and A. Börner, Organic Carbonates as Solvents in Synthesis and Catalysis, *Chem. Rev.*, 2010, **110**(8), 4554–4581, DOI: 10.1021/cr900393d.
10 F. Ouhib, L. Meabe and A. Mahmoud, *et al.*, Influence of the Cyclic versus Linear Carbonate Segments in the Properties and Performance of CO_2-Sourced Polymer Electrolytes for Lithium Batteries, *ACS Appl. Polym. Mater.*, 2020, **2**(2), 922–931, DOI: 10.1021/acsapm.9b01130.
11 R. Sun, Y. Liao and S.-T. Bai, *et al.*, Heterogeneous catalysts for CO_2 hydrogenation to formic acid/formate: from nanoscale to single atom, *Energy Environ. Sci.*, 2021, **14**(3), 1247–1285, DOI: 10.1039/D0EE03575K.
12 W. Zhang, Y. Hu and L. Ma, *et al.*, Progress and Perspective of Electrocatalytic CO_2 Reduction for Renewable Carbonaceous Fuels and Chemicals, *Adv. Sci.*, 2018, **5**(1), 1700275, DOI: 10.1002/advs.201700275.
13 X. Liu and L. Dai, Carbon-based metal-free catalysts, *Nat. Rev. Mater.*, 2016, **1**(11), 16064, DOI: 10.1038/natrevmats.2016.64.
14 H.-J. Zhu, M. Lu and Y.-R. Wang, *et al.*, Efficient electron transmission in covalent organic framework nanosheets for highly active electrocatalytic carbon dioxide reduction, *Nat. Commun.*, 2020, **11**(1), 497, DOI: 10.1038/s41467-019-14237-4.
15 D. Yadav, Subodh and S. K. Awasthi, Recent advances in the design, synthesis and catalytic applications of triazine-based covalent organic polymers, *Mater. Chem. Front.*, 2022, **6**(12), 1574–1605, DOI: 10.1039/D2QM00071G.

16 M. Jia, J. Li, J. Gu, L. Zhang and Y. Liu, Inquiry for the multifunctional design of metal–organic frameworks: in situ equipping additional open metal sites (OMSs) inducing high CO_2 capture/conversion abilities, *Mater. Chem. Front.*, 2021, **5**(3), 1398–1404, DOI: **10.1039/D0QM00813C**.

17 S. Meng, G. Li, P. Wang, M. He, X. Sun and Z. Li, Rare earth-based MOFs for photo/electrocatalysis, *Mater. Chem. Front.*, 2023, **7**(5), 806–827, DOI: **10.1039/D2QM01201D**.

18 B. B. Narzary, B. C. Baker, N. Yadav, V. D'Elia and C. F. J. Faul, Crosslinked porous polyimides: structure, properties and applications, *Polym. Chem.*, 2021, **12**(45), 6494–6514, DOI: **10.1039/D1PY00997D**.

19 M. R. Liebl and J. Senker, Microporous Functionalized Triazine-Based Polyimides with High CO_2 Capture Capacity, *Chem. Mater.*, 2013, **25**(6), 970–980, DOI: **10.1021/cm4000894**.

20 Y. Liao, J. Weber and C. F. J. Faul, Fluorescent Microporous Polyimides Based on Perylene and Triazine for Highly CO_2 -Selective Carbon Materials, *Macromolecules*, 2015, **48**(7), 2064–2073, DOI: **10.1021/ma501662r**.

21 D. Tian, H.-Z. Zhang and D.-S. Zhang, *et al.*, Li-ion storage and gas adsorption properties of porous polyimides (PIs), *RSC Adv.*, 2014, **4**(15), 7506, DOI: **10.1039/c3ra45563g**.

22 A. Roy, S. Mondal and A. Halder, *et al.*, Benzimidazole linked arylimide based covalent organic framework as gas adsorbing and electrode materials for supercapacitor application, *Eur. Polym. J.*, 2017, **93**, 448–457, DOI: **10.1016/j.eurpolymj.2017.06.028**.

23 J. Lv, Y.-X. Tan and J. Xie, *et al.*, Direct Solar-to-Electrochemical Energy Storage in a Functionalized Covalent Organic Framework, *Angew. Chem., Int. Ed.*, 2018, **57**(39), 12716–12720, DOI: **10.1002/anie.201806596**.

24 R. van der Jagt, A. Vasileiadis and H. Veldhuizen, *et al.*, Synthesis and Structure–Property Relationships of Polyimide Covalent Organic Frameworks for Carbon Dioxide Capture and (Aqueous) Sodium-Ion Batteries, *Chem. Mater.*, 2021, **33**(3), 818–833, DOI: **10.1021/acs.chemmater.0c03218**.

25 J.-D. Xiao, L.-G. Qiu, Y.-P. Yuan, X. Jiang, A.-J. Xie and Y.-H. Shen, Ultrafast microwave-enhanced ionothermal synthesis of luminescent crystalline polyimide nanosheets for highly selective sensing of chromium ions, *Inorg. Chem. Commun.*, 2013, **29**, 128–130, DOI: **10.1016/j.inoche.2012.12.028**.

26 Q. Fang, J. Wang and S. Gu, *et al.*, 3D Porous Crystalline Polyimide Covalent Organic Frameworks for Drug Delivery, *J. Am. Chem. Soc.*, 2015, **137**(26), 8352–8355, DOI: **10.1021/jacs.5b04147**.

27 Q. Li, R. Chen and Y. Guo, *et al.*, Fluorinated Linear Copolyimide Physically Crosslinked with Novel Fluorinated Hyperbranched Polyimide Containing Large Space Volumes for Enhanced Mechanical Properties and UV-Shielding Application, *Polymers*, 2020, **12**(1), 88, DOI: **10.3390/polym12010088**.

28 J. G. Kim, J. Lee, J. Lee, S. I. Jo and J. Y. Chang, A hierarchically porous polyimide composite prepared by one-step condensation reaction inside a sponge for heterogeneous catalysis, *Macromol. Res.*, 2017, **25**(6), 629–634, DOI: **10.1007/s13233-017-5122-9**.

29 W. Zhu, X. Wang and T. Li, *et al.*, Porphyrin-based porous polyimide polymer/Pd nanoparticle composites as efficient catalysts for Suzuki–Miyaura coupling reactions, *Polym. Chem.*, 2018, **9**(12), 1430–1438, DOI: **10.1039/C8PY00092A**.

30 T. Chen, W. Xiao, J. Yang, M. Qiu, C. Yi and Z. Xu, Polyimide-supported Cu/2,2,6,6-tetramethyl-1-piperidine-N-oxyl catalytic systems: Aromatic donor-acceptor interaction-directed cooperative catalysis, *J. Colloid Interface Sci.*, 2022, **622**, 202–208, DOI: **10.1016/j.jcis.2022.04.120**.

31 L. Wang, W. Chen and D. Zhang, *et al.*, Surface strategies for catalytic CO_2 reduction: from two-dimensional materials to nanoclusters to single atoms, *Chem. Soc. Rev.*, 2019, **48**(21), 5310–5349, DOI: **10.1039/C9CS00163H**.

32 G. Singh, J. Lee and A. Karakoti, *et al.*, Emerging trends in porous materials for CO2capture and conversion, *Chem. Soc. Rev.*, 2020, **49**(13), 4360–4404, DOI: **10.1039/d0cs00075b**.

33 B. B. Narzary, B. C. Baker and C. F. J. Faul, Selective CO_2 Electroreduction from Tuneable Naphthalene-Based Porous Polyimide Networks, *Adv. Mater.*, 2023, **35**(20), 2211795, DOI: **10.1002/adma.202211795**.

34 P. Cheng, X. Zhao and X. Zhan, Perylene Diimide-Based Oligomers and Polymers for Organic Optoelectronics, *Acc. Mater. Res.*, 2022, **3**(3), 309–318, DOI: **10.1021/accountsmr.1c00191**.

35 Y. Li, Y. A. Samad, K. Polychronopoulou, S. M. Alhassan and K. Liao, From biomass to high performance solar–thermal and electric–thermal energy conversion and storage materials, *J. Mater. Chem. A*, 2014, **2**(21), 7759–7765, DOI: **10.1039/C4TA00839A**.

36 K. S. W. Sing, D. H. Everett and R. A. W. Haul, *et al.*, Reporting Physisorption Data For Gas/Solid Systems with Special Reference to the Determination of Surface Area and Porosity, *Pure Appl. Chem.*, 1985, **57**(4), 603–619, DOI: **10.1351/pac198557040603**.

37 R. Walczak, A. Savateev and J. Heske, *et al.*, Controlling the strength of interaction between carbon dioxide and nitrogen-rich carbon materials by molecular design, *Sustainable Energy Fuels*, 2019, **3**(10), 2819–2827, DOI: **10.1039/C9SE00486F**.

38 H. M. Lee, I. S. Youn, M. Saleh, J. W. Lee and K. S. Kim, Interactions of CO_2 with various functional molecules, *Phys. Chem. Chem. Phys.*, 2015, **17**(16), 10925–10933, DOI: **10.1039/C5CP00673B**.

39 S. Bhunia, R. A. Molla, V. Kumari, S. M. Islam and A. Bhaumik, Zn(II) assisted synthesis of porous salen as an efficient heterogeneous scaffold for capture and conversion of CO_2, *Chem. Commun.*, 2015, **51**(86), 15732–15735, DOI: **10.1039/C5CC06868A**.

40 J. Chen, H. Li, M. Zhong and Q. Yang, Hierarchical mesoporous organic polymer with an intercalated metal complex for the efficient synthesis of cyclic carbonates from flue gas, *Green Chem.*, 2016, **18**(24), 6493–6500, DOI: **10.1039/C6GC02367C**.

41 J. Liang, Y. B. Huang and R. Cao, Metal–organic frameworks and porous organic polymers for sustainable fixation of carbon dioxide into cyclic carbonates, *Coord. Chem. Rev.*, 2019, **378**, 32–65, DOI: **10.1016/j.ccr.2017.11.013**.

42 O. Buyukcakir, S. H. Je, S. N. Talapaneni, D. Kim and A. Coskun, Charged Covalent Triazine Frameworks for CO_2 Capture and Conversion, *ACS Appl. Mater. Interfaces*, 2017, **9**(8), 7209–7216, DOI: **10.1021/acsami.6b16769**.

43 J. Roeser, K. Kailasam and A. Thomas, Covalent Triazine Frameworks as Heterogeneous Catalysts for the Synthesis of Cyclic and Linear Carbonates from Carbon Dioxide and Epoxides, *ChemSusChem*, 2012, **5**(9), 1793–1799, DOI: **10.1002/cssc.201200091**.

44 S. Ding, L. Sun and X. Ma, *et al.*, Microporous Polymeric Spheres as Highly Efficient and Metal-Free Catalyst for the Cycloaddition of CO_2 to Cyclic Organic Carbonates at Ambient Conditions, *Catal Lett.*, 2020, **150**(10), 2970–2977, DOI: **10.1007/s10562-020-03206-y**.

45 Y. Zhi, P. Shao and X. Feng, *et al.*, Covalent organic frameworks: efficient, metal-free, heterogeneous organocatalysts for chemical fixation of CO_2 under mild conditions, *J. Mater. Chem. A*, 2018, **6**(2), 374–382, DOI: **10.1039/C7TA08629F**.

46 B. Yu and L. N. He, Upgrading carbon dioxide by incorporation into heterocycles, *ChemSusChem*, 2015, **8**(1), 52–62, DOI: **10.1002/cssc.201402837**.

47 X. D. Lang and L. N. He, Green Catalytic Process for Cyclic Carbonate Synthesis from Carbon Dioxide under Mild Conditions, *Chem. Rec.*, 2016, **16**, 1337–1352, DOI: **10.1002/tcr.201500293**.

48 T. Kimura, K. Kamata and N. Mizuno, A bifunctional tungstate catalyst for chemical fixation of CO_2 at atmospheric pressure, *Angew. Chem., Int. Ed.*, 2012, **51**(27), 6700–6703, DOI: **10.1002/anie.201203189**.

49 Y. Zhang and S. N. Riduan, Functional porous organic polymers for heterogeneous catalysis, *Chem. Soc. Rev.*, 2012, **41**(6), 2083–2094, DOI: **10.1039/C1CS15227K**.

50 G. H. Gunasekar, J. Shin, K.-D. Jung, K. Park and S. Yoon, Design Strategy toward Recyclable and Highly Efficient Heterogeneous Catalysts for the Hydrogenation of CO_2 to Formate, *ACS Catal.*, 2018, **8**(5), 4346–4353, DOI: **10.1021/acscatal.8b00392**.

51 X. Zhang, B. Qiu and Y. Zou, *et al.*, Green synthesized cobalt-bipyridine constructed conjugated microporous polymer: An efficient heterogeneous catalyst for cycloaddition of epoxides via CO2 fixation under ambient conditions, *Microporous Mesoporous Mater.*, 2021, **319**, 110758, DOI: **10.1016/j.micromeso.2020.110758**.

52 X. Zhang, J. Wang and Y. Bian, *et al.*, A novel conjugated microporous polymer microspheres comprising cobalt porphyrins for efficient catalytic CO_2 cycloaddition under ambient conditions, *J. CO_2* Util., 2022, **58**, 101924, DOI: **10.1016/j.jcou.2022.101924**.

53 F. Zhou, Q. Deng, N. Huang, W. Zhou and W. Deng, CO_2 Fixation into Cyclic Carbonates by a Zn-Salen Based Conjugated Microporous Polymer, *ChemistrySelect*, 2020, **5**(34), 10516–10520, DOI: **10.1002/slct.202001538**.

54 Y. Lu, Z. Chang and S. Zhang, *et al.*, Porous organic polymers containing zinc porphyrin and phosphonium bromide as bifunctional catalysts for conversion of carbon dioxide, *J. Mater. Sci.*, 2020, **55**(26), 11856–11869, DOI: **10.1007/s10853-020-04851-9**.

55 R. Sharma, A. Bansal, C. N. Ramachandran and P. Mohanty, A multifunctional triazine-based nanoporous polymer as a versatile organocatalyst for CO_2 utilization and C–C bond formation, *Chem. Commun.*, 2019, **55**(77), 11607–11610, DOI: **10.1039/C9CC04975D**.

56 C. Lu, J. Yang and S. Wei, *et al.*, Atomic Ni Anchored Covalent Triazine Framework as High Efficient Electrocatalyst for Carbon Dioxide Conversion, *Adv. Funct. Mater.*, 2019, **29**(10), 1806884, DOI: **10.1002/adfm.201806884**.

57 D.-H. Yang, Y. Tao, X. Ding and B.-H. Han, Porous organic polymers for electrocatalysis, *Chem. Soc. Rev.*, 2022, **51**(2), 761–791, DOI: **10.1039/D1CS00887K**.

58 J. Li, Y. Kuang and Y. Meng, *et al.*, Electroreduction of CO_2 to Formate on a Copper-Based Electrocatalyst at High Pressures with High Energy Conversion Efficiency, *J. Am. Chem. Soc.*, 2020, **142**(16), 7276–7282, DOI: **10.1021/jacs.0c00122**.

59 W. Guo, S. Liu and X. Tan, *et al.*, Highly Efficient CO2 Electroreduction to Methanol through Atomically Dispersed Sn Coupled with Defective CuO Catalysts, *Angew. Chem., Int. Ed.*, 2021, **60**(40), 21979–21987, DOI: **10.1002/anie.202108635**.

60 J. Chen, W. Yan and E. J. Townsend, *et al.*, Tunable Surface Area, Porosity, and Function in Conjugated Microporous Polymers, *Angew. Chem., Int. Ed.*, 2019, **58**(34), 11715–11719, DOI: **10.1002/anie.201905488**.

61 J. Chen, T. Qiu, W. Yan and C. F. J. Faul, Exploiting Hansen solubility parameters to tune porosity and function in conjugated microporous polymers, *J Mater Chem A*, 2020, **8**(43), 22657–22665, DOI: **10.1039/D0TA05563H**.